NUCL SCI TECH (2018) 29:116
https://doi.org/10.1007/s41365-018-0452-7

J/ψ production in p+p and p+Pb collisions at ultrarelativistic energies

Hong-Min Wang[1] · Zhao-Yu Hou[2] · Xiu-Ting Wang[1] · Xian-Jing Sun[3]

Received: 22 February 2018 / Revised: 14 April 2018 / Accepted: 16 April 2018 / Published online: 4 July 2018

Abstract The production of J/ψ mesons in p+p and p+Pb collisions is studied in the framework of color-glass condensate together with a simple color evaporation model. Considering the nuclear effects with the Glauber–Gribov approach, we calculate the cross section and the nuclear modification factor of forward J/ψ production in p+Pb collisions at $\sqrt{s} = 5.02$ TeV. Then, the backward J/ψ production in p+Pb collisions at $\sqrt{s} = 8.16$ TeV is also analyzed. In our calculation, the phenomenology KLR-AdS/CFT model and the rcBK approach, which are valid at a small x, are used to calculate the three-point function. It is shown that the theoretical results fit well with the experimental data from ALICE and LHCb.

Keywords Color-glass condensate · Forward J/ψ production · Glauber–Gribov approach

This work was supported by the Natural Science Foundation of Hebei Province (A2012210043).

✉ Hong-Min Wang
whmw@sina.com

1 Physics Department, Academy of Army Armored Forces of PLA, Beijing 100072, China

2 Physics Graduate School, Shijiazhuang Railway Institute, Shijiazhuang 050043, China

3 Institute of High Energy Physics, Chinese Academy of Sciences, Beijing 100049, China

1 Introduction

The production of forward J/ψ mesons in proton–proton (p+p) and proton–nucleus (p+A) collisions can provide valuable insight into the gluon saturation physics and strong color fields at a small x. Thus, this subject has received much attention on nuclear theory sides in recent years [1–5]. There are two stages for J/ψ production. The first stage is the $c\bar{c}$ pair production in p+p and p+A collisions. The color-glass condensate (CGC) theory, which consider the p+p (A) as a dilute-dense system, is an effective method to study the $c\bar{c}$ pair production. According to the CGC theory, the $c\bar{c}$ pair production comes from two processes at leading order. One process is that the gluon from the incoming proton splits into a $c\bar{c}$ pair before multiple scattering with the target, and the other process is that the incoming gluon multiplies scatters with the target nucleus first and then splits into the $c\bar{c}$ pair. The second stage is the $c\bar{c}$ pair producing the J/ψ meson. This process can be described with the simple color evaporation model (CEM) [6, 7]. In this model, the color of the $c\bar{c}$ pair is assumed to be "evaporated" away in the form of a soft gluon, and then all the $c\bar{c}$ pair are assumed to become the J/ψ mesons with a fixed fraction below the D-meson threshold.

In the CGC framework, the dipole amplitude is the key ingredient to compute the cross section for $c\bar{c}$ pair production. At Large Hadron Collider (LHC) energies, the value of Bjorken-x for $c\bar{c}$ pair production in p+p (Pb) collisions will be down to 10^{-6}. At this x domain, the common phenomenological saturation models, such as the CGC model [8], the Soyez model [9], and the Golec-Biernat and Wüsthoff (GBW) model [10], are not valid. Recently, it is more popular to use the running coupling

Balitsky–Kovchegov (rcBK) equation for the dipole amplitude [1–3]. Unfortunately, there is a Fourier transform to obtain the unintegrated gluon distribution (UGD) from the dipole amplitude. Because the Fourier transform is an oscillatory integral [11], it is too difficult to ensure the accuracy of the theoretical results with the rcBK approach, especially at large p_{T}. Here, we will introduce the phenomenological model proposed by Kovchegov, Lu, and Rezaeian (KLR) [12, 13]. This model is depended on the anti-de Sitter space/conformal field theory (AdS/CFT) approach, and proved very valid at a small Bjorken-x domain ($10^{-4}\sim 10^{-6}$). Furthermore, an analytic formula of the UGD can be obtained from the dipole amplitude given by the KLR-AdS/CFT model. Thus, the accuracy of the theoretical results can be ensured. In this paper, we will use the rcBK approach and the KLR-AdS/CFT model to investigate the J/ψ production in p+p and p+Pb collisions at LHC energies.

In order to study the nuclear suppression of forward J/ψ production in p+A collisions, the nuclear effects should be considered. A simple method to consider nuclear effects is by relating the saturation scale of a heavy nucleus, $Q_{\mathrm{sA}}^2(x)$, to that of a proton, $Q_{\mathrm{sp}}^2(x)$, through formula $Q_{\mathrm{sA}}^2(x) = A^{1/3}Q_{\mathrm{sp}}^2(x)$ [14]. In the frame of the recently published papers [15, 16], the authors consider impact parameter (b) dependence on the saturation scale using CGC approximation and investigate the nuclear configurational entropy. The results match the fitted experimental data at 1%. Besides, Refs. [17–20] offered a quantitative study of quarkonia radially excited S-wave states and paved a way into which bottomonium and charmonium were studied from the point of view of the configurational entropy in the AdS/QCD correspondence as well as in the refinement of topological defects. Thus, for getting more reliable theoretical results, the impact parameter, b, dependence of the nuclear saturation scale should be considered. In this paper, the nuclear effects are considered in the Glauber–Gribov approach [21, 22]. We assume that the dipole-nucleus scattering amplitude relate to the dipole-proton case by the formula $Q_{\mathrm{sA}}^2(x) = N_{\mathrm{part,A}}(b)Q_{\mathrm{sp}}^2(x)$, where $N_{\mathrm{part,A}}(b)$ is the number of participating nucleons in p+A collisions.

This paper is organized as follows. In Sect. 2, we introduce the theoretical formalism for $c\bar{c}$ pair production in the large N_{c} limit. Then, we give the method of calculating the differential cross section for J/ψ production in Sect. 3. In Sect. 4, we give the theoretical results and compare them with the recent experimental data from ALICE and LHCb.

2 Quark pair production cross section in the large N_c limit

In the CGC framework, the cross section of quark pair production with the transverse momentum, $\mathbf{p}_{\mathrm{T}}(\mathbf{q}_{\mathrm{T}})$, and rapidity, $y_{\mathrm{p}}(y_{\mathrm{q}})$ of the quark (anti-quark) can be written as [1]

$$\frac{d\sigma_{q\bar{q}}}{d^2\mathbf{p}_{\mathrm{T}}d^2\mathbf{q}_{\mathrm{T}}dy_{\mathrm{p}}dy_{\mathrm{q}}} = \frac{\alpha_s^2}{16\pi^2 C_{\mathrm{F}}}\int\frac{d^2\mathbf{k}_{\mathrm{T}}}{(2\pi)^4}\frac{\Xi_{\mathrm{coll}}(\mathbf{p}_{\mathrm{T}}+\mathbf{q}_{\mathrm{T}},\mathbf{k}_{\mathrm{T}})}{(\mathbf{p}_{\mathrm{T}}+\mathbf{q}_{\mathrm{T}})^2}$$
$$\phi_{\mathrm{A},y_2}^{\mathrm{qq,g}}(\mathbf{p}_{\mathrm{T}}+\mathbf{q}_{\mathrm{T}},\mathbf{k}_{\mathrm{T}})x_1G_{\mathrm{p}}(x_1,Q^2), \tag{1}$$

where $C_{\mathrm{F}} = (N_{\mathrm{c}}^2-1)/(2N_{\mathrm{c}})$ with $N_{\mathrm{c}} = 3$, and x_1 and x_2 are the longitudinal momentum fractions of the gluons from the projectile and target, respectively. Ξ_{coll} is the "hard matrix element," which can be given as Ref. [23]

$$\Xi_{\mathrm{coll}} = \Xi_{\mathrm{coll}}^{q\bar{q},q\bar{q}} + \Xi_{\mathrm{coll}}^{qq,g} + \Xi_{\mathrm{coll}}^{g,g}, \tag{2}$$

where $\Xi_{\mathrm{coll}}^{q\bar{q},q\bar{q}}$ is the term of a quark pair scattering off the nuclei, $\Xi_{\mathrm{coll}}^{g,g}$ is the term before the gluon splitting into a quark pair, and $\Xi_{\mathrm{coll}}^{q\bar{q},g}$ corresponds to the interference between the quark and gluon. The explicit expressions are

$$\Xi_{\mathrm{coll}}^{q\bar{q},q\bar{q}} = \frac{8p^+q^+}{(p^++q^+)^2(\mathbf{a}_{\mathrm{T}}^2+m_{\mathrm{c}}^2)^2}\left[m_{\mathrm{c}}^2 + \frac{(p^+)^2+(q^+)^2}{(p^++q^+)^2}\mathbf{a}_{\mathrm{T}}^2\right], \tag{3}$$

$$\Xi_{\mathrm{coll}}^{q\bar{q},g} = -\frac{16}{(p+q)^2(\mathbf{a}_{\mathrm{T}}^2+m_{\mathrm{c}}^2)} \times\left[m_{\mathrm{c}}^2 + \frac{(p^+)^2+(q^+)^2}{(p^++q^+)^3}\mathbf{a}_{\mathrm{T}}\cdot(p^+\mathbf{q}_{\mathrm{T}}-q^+\mathbf{p}_{\mathrm{T}})\right], \tag{4}$$

$$\Xi_{\mathrm{coll}}^{g,g} = \frac{8}{(p+q)^4}\left[(p+q)^2 - \frac{2}{(p^++q^+)^2}(p^+\mathbf{q}_{\mathrm{T}}-q^+\mathbf{p}_{\mathrm{T}})^2\right], \tag{5}$$

with $\mathbf{a}_{\mathrm{T}} \equiv \mathbf{q}_{\mathrm{T}} - \mathbf{k}_{\mathrm{T}}$. $x_1G_{\mathrm{p}}(x_1,Q^2)$ is the collinear gluon distribution function of the proton. In this work, we use the CTEQ6 LO parametrization [24].

The three-point function of the nucleus in Eq. (1) can be expressed as

$$\phi_{\mathrm{A},y_2}^{\mathrm{qq,g}}(\mathbf{l}_{\mathrm{T}},\mathbf{k}_{\mathrm{T}}) = \int d^2\mathbf{b}\frac{N_{\mathrm{c}}\mathbf{l}_{\mathrm{T}}^2}{4\alpha_s}S_{\mathrm{Y}}(\mathbf{k}_{\mathrm{T}})S_{\mathrm{Y}}(\mathbf{l}_{\mathrm{T}}-\mathbf{k}_{\mathrm{T}}), \tag{6}$$

where $\mathbf{b}$ is the impact parameter and $\mathbf{l}_{\mathrm{T}} = \mathbf{p}_{\mathrm{T}} + \mathbf{q}_{\mathrm{T}}$. The UGD can be obtained by a Fourier transform [11, 25]

$$S_{\mathrm{Y}}(\mathbf{k}_{\mathrm{T}}) = \int d^2\mathbf{r}_{\mathrm{T}}e^{i\mathbf{k}_{\mathrm{T}}\cdot\mathbf{r}_{\mathrm{T}}}S_{\mathrm{Y}}(\mathbf{r}_{\mathrm{T}}) = \int\frac{dr_{\mathrm{T}}}{r_{\mathrm{T}}}J_0(r_{\mathrm{T}}k)S_{\mathrm{Y}}(\mathbf{r}_{\mathrm{T}}), \tag{7}$$

where $S_{\rm Y}(\mathbf{r}_{\rm T})$ is the dipole amplitude and J_0 is the spherical bessel function of the first kind.

In this paper, the rcBK approach and the KLR-AdS/CFT model are used for $S_{\rm Y}(\mathbf{r}_{\rm T})$. In the rcBK approach, the dipole scattering amplitude can be given by Ref. [25]

$$\frac{\partial S(\mathbf{r}_{\rm T})}{\partial Y} = \int {\rm d}\mathbf{r}_{1\rm T} K^{\rm Bal}(\mathbf{r}_{\rm T},\mathbf{r}_{1\rm T},\mathbf{r}_{2\rm T})[S(\mathbf{r}_{1\rm T}) + S(\mathbf{r}_{2\rm T}) - S(\mathbf{r}_{\rm T}) - S(\mathbf{r}_{1\rm T})S(\mathbf{r}_{2\rm T})], \tag{8}$$

where $K^{\rm Bal}(\mathbf{r}_{\rm T},\mathbf{r}_{1\rm T},\mathbf{r}_{2\rm T})$ is the kernel for the running term, and the GBW ansatz is used for the initial conditions of the dipole scattering amplitude

$$S^{\rm GBW}(\mathbf{r}_{\rm T}) = 1 - \exp\left[-\left(\frac{r_{\rm T}^2 Q_{s0}^2}{4}\right)^{\gamma}\right] \tag{9}$$

with $\gamma = 1$ and $Q_{s0}^2 = 0.24$ GeV^2. The dipole-proton scattering amplitude in the KLR-AdS/CFT model can be written as Ref. [12, 13]

$$S_{\rm Y}^{\rm AdS}(\mathbf{r}_{\rm T}) = 1 - \exp\left[-rQ_{\rm s,p}^{AdS}(x)/(2\sqrt{2})\right], \tag{10}$$

where the saturation scale is given by

$$Q_{\rm s,p}^{\rm AdS}(x) = \frac{2A_0 x}{M_0^2(1-x)\pi}\left(\frac{1}{\rho_{\rm m}^3} + \frac{2}{\rho_{\rm m}} - 2M_0\sqrt{\frac{1-x}{x}}\right), \tag{11}$$

with

$$\rho_{\rm m} = \begin{cases} \left(\frac{1}{3m}\right)^{1/4}\sqrt{2\cos(\frac{\theta}{3})} & : m \leq \frac{4}{27} \\ \sqrt{\frac{1}{3m\Delta} + \Delta} & : m > \frac{4}{27} \end{cases},$$

$$\Delta = \left[\frac{1}{2m} - \sqrt{\frac{1}{4m^2} - \frac{1}{27m^3}}\right]^{1/3},$$

$$m = \frac{M_0^4(1-x)^2}{x^2},$$

$$\cos\theta = \sqrt{\frac{27m}{4}},$$

$$A_0 = \sqrt{\lambda_{\rm YM}}\,{\rm GeV}.$$

Here, we choose $\lambda_{\rm YM} = 20$ and $M_0 = 6.16 \times 10^{-3}$, which are obtained from a fit to the HERA data.

For p+A collisions, the saturation scale of the nucleus can be given by Ref. [21, 22]

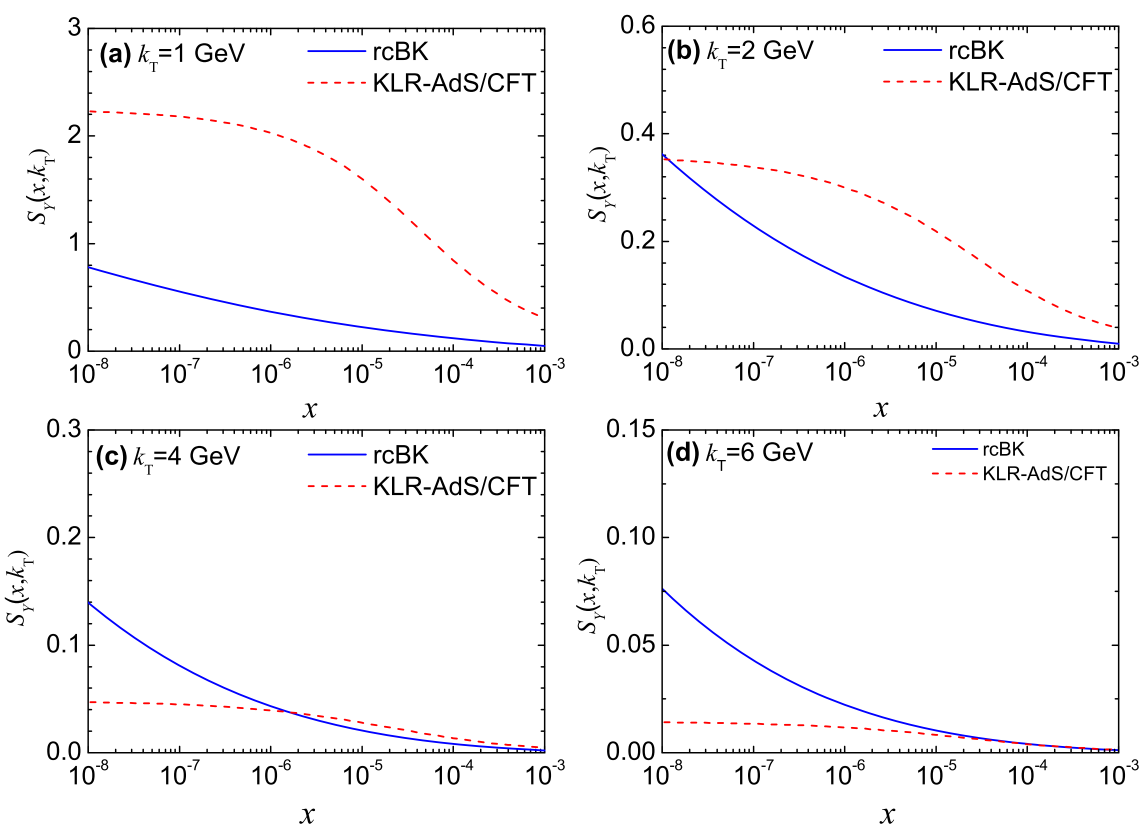

Fig. 1 (Color online) The UGD $S_{\rm Y}(x, k_{\rm T})$ versus x with the rcBK approach (solid curves) and the KLR-AdS/CFT model (dashed curves) at $k_{\rm T}$ = 1 GeV (**a**), 2 GeV (**b**), 4 GeV (**c**) and 6 GeV (**d**)

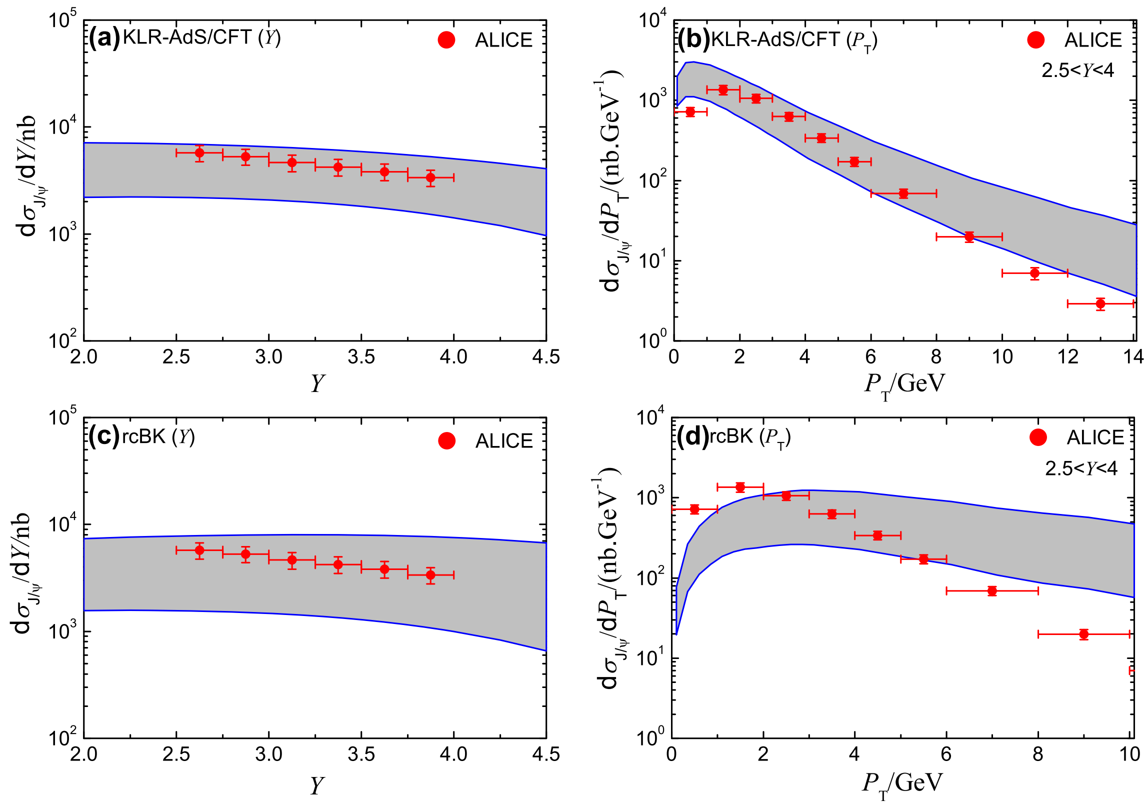

Fig. 2 (Color online) Differential cross section for J/ψ production in p+p collisions at $\sqrt{s} = 7$ TeV as a function of Y (**a**,**c**) and P_{T} (**b**,**d**) with the KLR-AdS/CFT model (**a**,**b**) and the rcBK approach (**c**,**d**). The data come from ALICE [30]

$$Q^2_{\mathrm{s,A}}(x) = N_{\mathrm{part,A}} Q^2_{\mathrm{s,p}}(x), \tag{12}$$

where the participating nucleons in the collisions, $N_{\mathrm{part},A}$, can be given by a convolution of the thickness function of the proton and nucleus [26]. For the thickness function of the nucleus, we use the Woods–Saxon form [27]

$$T_{\mathrm{A}}(\mathbf{b}) = \int \mathrm{d}z \frac{\rho_0}{1+\exp(\frac{r-R}{a})}, \tag{13}$$

where ρ_0 is the nucleon density in the center of the nucleus and R is the nuclear radius [26]. For the proton, the Gaussian form is used [28]

$$T_{\mathrm{p}}(\mathbf{b}) = \frac{e^{-b^2/(2B)}}{2\pi B} \tag{14}$$

with $B = \frac{\sigma_{\mathrm{in}}}{14.30}\ \mathrm{fm}^2$.

3 Differential cross section in terms of the J/ψ variate

In order to compare with the experimental data, we should express the cross section in Eq. (1) in terms of the variate of J/ψ, which are the invariant mass, M^2, the transverse momentum, P_{T}, and rapidity, Y. The relation equation can be written as Ref. [29]

$$\frac{\mathrm{d}\sigma}{\mathrm{d}M^2\mathrm{d}^2\mathbf{P}_{\mathrm{T}}\mathrm{d}Y} = \int_0^{\sqrt{M^2/4-m_c^2}} \mathrm{d}\tilde{q} \int_0^{2\pi} \mathrm{d}\phi \frac{\tilde{q}\gamma_x}{\omega_{\mathrm{p}}\omega_{\mathrm{q}} \mid \sinh(y_{\mathrm{p}} - yq) \mid} \frac{\mathrm{d}\sigma}{\mathrm{d}^2\mathbf{p}_{\mathrm{T}}\mathrm{d}^2\mathbf{q}_{\mathrm{T}}\mathrm{d}y_{\mathrm{p}}\mathrm{d}y_{\mathrm{q}}}, \tag{15}$$

where $\omega_{\mathrm{q}} = \sqrt{\mathbf{q}^2_{\mathrm{T}} + m^2_{\mathrm{c}}}$ ($\omega_{\mathrm{p}} = \sqrt{\mathbf{p}^2_{\mathrm{T}} + m^2_{\mathrm{c}}}$) is the transverse masses of the quark (anti-quark). $\tilde{\mathbf{q}}$ is the quark (or anti-quark) transverse momentum in the center of mass system of the quark pair and ϕ is the angle between $\tilde{\mathbf{q}}$ and the x-axis. In Eq. (15), the momenta of the quark and anti-quark are given by

$$q^\mu = \mathbf{L}_{\mathrm{z}}(\beta_z)^\mu_\nu \mathbf{L}_{\mathrm{x}}(\beta_{\mathrm{x}})^\nu_\sigma q^\sigma_{\mathrm{cm}}$$
$$p^\mu = \mathbf{L}_{\mathrm{z}}(\beta_z)^\mu_\nu \mathbf{L}_{\mathrm{x}}(\beta_{\mathrm{x}})^\nu_\sigma p^\sigma_{\mathrm{cm}}, \tag{16}$$

where the momenta in the center of mass system of the quark pair q^σ_{cm} and p^σ_{cm} can be given as

$$q^\sigma_{\mathrm{cm}} = \left(\frac{M}{2}, \tilde{q}\cos\phi, \tilde{q}\sin\phi, \sqrt{M^2/4 - m^2_{\mathrm{c}} - \tilde{q}^2}\right)$$

and

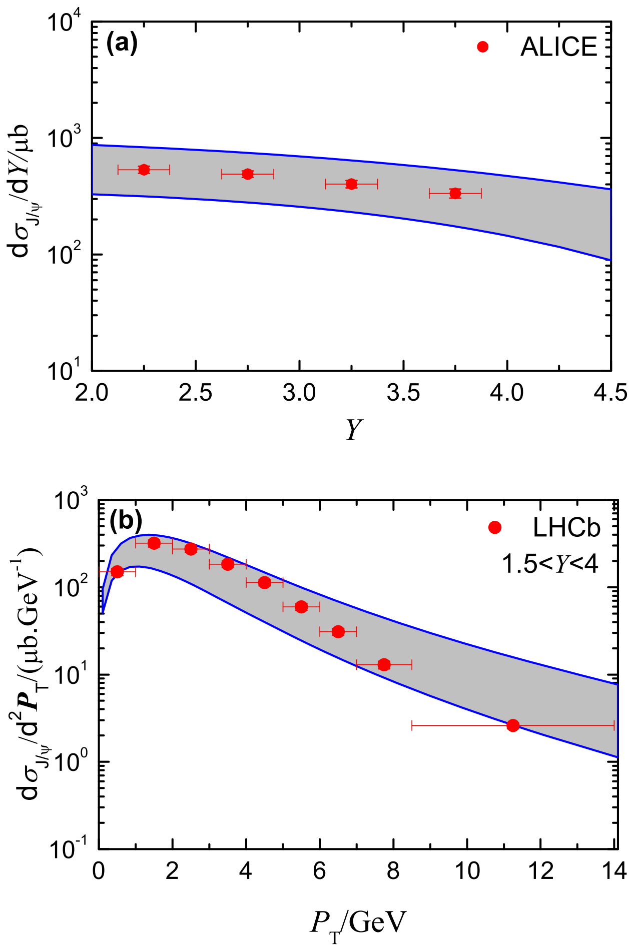

Fig. 3 (Color online) Differential cross section for J/ψ production in p+Pb collisions as a function of Y (**a**) and P_T (**b**) at $\sqrt{s} = 5.02$ TeV. The data come from ALICE [31] and LHCb [32]

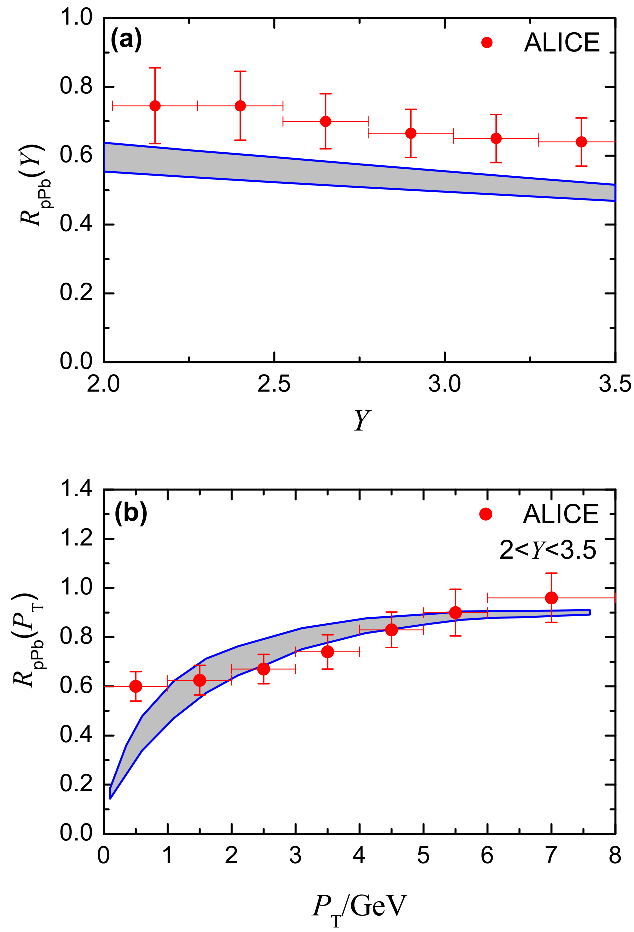

Fig. 4 (Color online) Nuclear modification factor for J/ψ production in p+Pb collisions as a function of Y (**a**) and P_T (**b**) at $\sqrt{s} = 5.02$ TeV. The data come from ALICE [31, 33]

$$p^{\sigma}_{\rm cm} = \left(\frac{M}{2}, -\tilde{q}\cos\phi, -\tilde{q}\sin\phi, -\sqrt{M^2/4 - m_c^2 - \tilde{q}^2}\right). \tag{17}$$

In Eq. (16), $\mathbf{L}_x(\beta_x)$ and $\mathbf{L}_z(\beta_z)$ are the Lorentz boosts in the x-axis and z-axis, respectively. $\beta_x = |\mathbf{P}_T|/\sqrt{M^2 + \mathbf{P}_T^2}$ and $\beta_z = \tanh(Y)$.

To calculate the cross section of J/ψ, we will use the simple color evaporation model [6, 7]. This model assumes that all $c\bar{c}$ pairs produced become J/ψ mesons below the D-meson threshold. This can be expressed as

$$\frac{d\sigma_{J/\psi}}{dYd^2\mathbf{P}_T} = F_{J/\psi}\int_{4m_c^2}^{4m_D^2} dM^2 \frac{d\sigma}{dM^2 d^2\mathbf{P}_T dY}, \tag{18}$$

where $F_{J/\psi}(= 0.01 - 0.05)$ is a nonperturbative quantity representing the probability that a $c\bar{c}$ pair will become a J/ψ [23].

4 Results and discussion

For the UGD of the KLR-AdS/CFT model, an analytic form can be obtained from Eq. (7)

$$S_Y(x, \mathbf{k}_T) = \frac{32\pi}{[Q^{\rm AdS}_{s,p}(x)]^2} \frac{1}{\{1 + 16k_T^2/[Q^{\rm AdS}_{s,p}(x)]^2\}^{3/2}}. \tag{19}$$

The UGD $S_Y(x, \mathbf{k}_T)$ versus x at $k_T = 1$ GeV (a), 2 GeV (b), 4 GeV (c), and 6 GeV (d) are shown in Fig. 1. The solid and dashed curves are the results of the rcBK approach and the KLR-AdS/CFT model, respectively. It is shown that the results of the KLR-AdS/CFT model are larger than that of the rcBK approach at small k_T, but the results are just the opposite at large k_T. It is also shown that the results of the KLR-AdS/CFT model are obviously independent of Bjorken-x when x is small.

In Fig. 2, we give the results for the production cross section of J/ψ in p+p collisions versus Y (a,c) and P_T (b,d) at a center of mass energy $\sqrt{s} = 7$ TeV . Figure 2a,b and c,d is the results of the KLR-AdS/CFT model and the rcBK

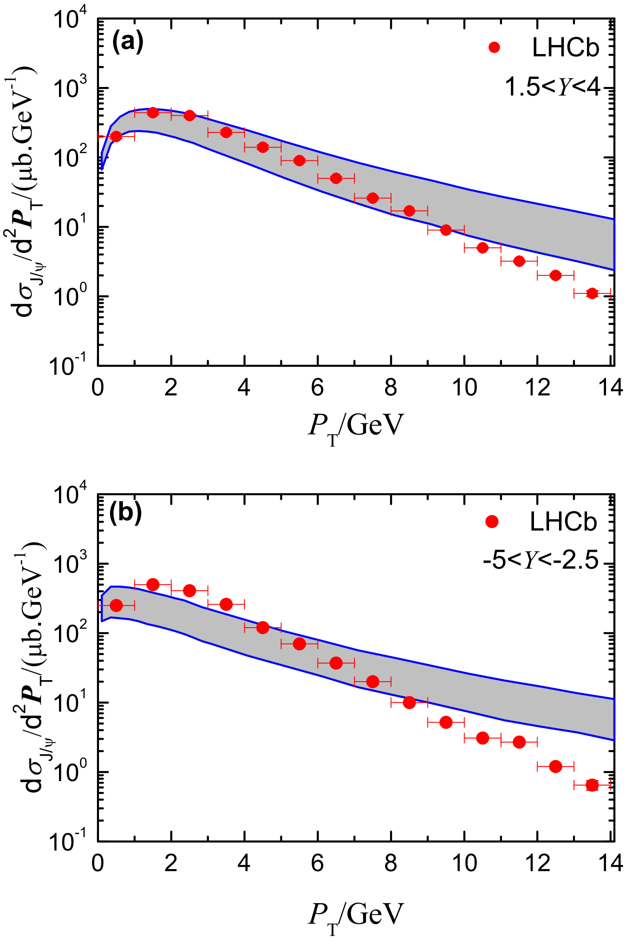

Fig. 5 Differential cross section for J/ψ production versus P_T at forward (**a**) and backward (**b**) rapidity in p+Pb collisions at $\sqrt{s} = 8.16$ TeV. The data are from LHCb [34]

approach, respectively. The uncertainty band includes the variation of the factorization scale between $2M_T$ and $M_T/2$ with $M_T = \sqrt{M^2 + P_T^2}$. The charm quark mass is taken as 1.2 GeV. The data come from ALICE [30]. The integral range in Fig. 2b,d is $2.5 < Y < 4$. For the KLR-AdS/CFT model, as shown in Fig. 2a,b, the theoretical results fit well with the experimental data except at a very large transverse momentum of J/ψ. The reason is that the CGC theory is not very accurate at a very large P_T. In Fig. 2c,d, it is shown that the normalization uncertainty for the results of the rcBK approach is larger than that of the KLR-AdS/CFT model. It is also shown that the curve in Fig. 2d is not smooth enough. This is because there is a Fourier transform in obtaining the UGD, as shown in Eq. (7). Because the Fourier transform is an oscillatory integral, it is very difficult to ensure the correctness of the results for the rcBK approach, especially at a large P_T. Thus, we will only give the results of the KLR-AdS/CFT model in p+Pb collisions.

Using Eq. (12), we show the differential cross section of J/ψ production versus Y (a) and P_T (b) in p+Pb collisions at a center of mass energy of $\sqrt{s} = 5.02$ TeV in Fig. 3. The theory uncertainty results are obtained by the same method as in Fig. 2, and the data come from ALICE [31] and LHCb [32]. The integral range in Fig. 3b is $1.5 < Y < 4$. It is shown that the theoretical results fit well with the experimental data. Here, there is only one experimental datum at large P_T (=8.5-14) GeV. If there are more data, the deviation of the theory results and the experimental data at large P_T may be the same as in Fig. 2.

In order to compare with experimental data, we introduce the nuclear modification factor

$$R_{pA}(Y) = \frac{1}{A}\frac{\langle d\sigma/dY\rangle|_{pA}}{\langle d\sigma/dY\rangle|_{pp}}, \tag{20}$$

and

$$R_{pA}(P_T) = \frac{1}{A}\frac{\langle d\sigma/d^2\mathbf{P}_T\rangle|_{pA}}{\langle d\sigma/d^2\mathbf{P}_T\rangle|_{pp}}, \tag{21}$$

where $\langle d\sigma/dY\rangle = \int d^2\mathbf{P}_T \frac{d\sigma}{d^2\mathbf{P}_T dY}$ and $\langle d\sigma/d^2\mathbf{P}_T\rangle = \int dY \frac{d\sigma}{d^2\mathbf{P}_T dY}$. In Fig. 4, we show the nuclear modification factor versus Y (a) and $\mathbf{P}_T$ (b) at $\sqrt{s} = 5.02$ TeV. The experimental data come from ALICE [31, 33]. In Figs. 2 and 3, it is shown that the theoretical results have a large uncertain region. Thus, although the theoretical results can describe the J/ψ cross section versus Y in p+p and p+Pb collisions, as shown in Fig. 4a, their ratios can't fit well with the data of $R_{pPb}(Y)$. In Fig. 4b, it is shown that the theoretical results fit the data well except at very low P_T.

In Fig. 5, we analyze the J/ψ production in p+Pb collisions at forward (a) and backward (b) rapidity at the center of mass energy of $\sqrt{s} = 8.16$ TeV. The integral ranges of rapidity are $1.5 < Y < 4$ and $-5 < Y < -2.5$ for Fig. 5a, b, respectively. The theory uncertainty results are the same as in Fig. 2 and the data come from the recent results of LHCb [34]. It is shown that the theoretical results at backward rapidity do not fit well with the data, especially at large P_T. Because the Bjorken-x is very large at backward rapidity, the CGC theory is not very effective in this rapidity range. The commonly called cold nuclear effect is an effective method to study J/ψ production at backward rapidity [6].

In summary, we have investigated forward J/ψ production in p+p and p+Pb collisions at LHC energies in the CGC framework together with the CEM. Considering the transverse distribution of the proton and nucleus, the theoretical results are in good agreement with the data from ALICE and LHCb with the analytic UGD from the KLR-AdS/CFT model. Unfortunately, there are still some deviations between the theoretical results and the data especially at large P_T. Thus, we should give a further study on this subject in the future.

References

1. H. Fujii, K. Watanabe, Leptons from heavy-quark semileptonic decay in pA collisions within the CGC framework. Nucl. Phys. A **951**, 45 (2016). https://doi.org/10.1016/j.nuclphysa.2016.03.045
2. B. Ducloue, T. Lappi, H. Mantysaari, Centrality-dependent forward J/ψ production in high energy proton–nucleus collisions. EPJ Web Conf. **112**, 04002 (2016). https://doi.org/10.1051/epjconf/201611204002
3. Y.Q. Ma, R. Venugopalan, H.F. Zhang, J/ψ production and suppression in high-energy proton–nucleus collisions. Phys. Rev. D **92**, 071901 (2015). https://doi.org/10.1103/PhysRevD.92.071901
4. H. Fujii, K. Watanabe, Nuclear modification of forward D production in pPb collisions at the LHC. arXiv:1706.06728
5. Y.M. Shabelski, A.G. Shuvaev, I.V. Surnin, Heavy quark production in k_t factorization approach at LHC energies. Int. J. Mod. Phys. A **33**, 1850003 (2018). https://doi.org/10.1142/S0217751X18500033
6. H.M. Wang, X.J. Sun, B.A. Zhang, x_F(or y)-dependence of nuclear absorption and energy loss effects on J/ψ production. Commun. Theor. Phys. **52**, 1049 (2009). https://doi.org/10.1088/0253-6102/52/6/14
7. R. Vogt, Shadowing and absorption effects on J/ψ production in dA collisions. Phys. Rev. C **71**, 054902 (2005). https://doi.org/10.1103/PhysRevC.71.054902
8. E. Iancu, K. Itakura, S. Munier, Saturation and BFKL dynamics in the HERA data at small-x. Phys. Lett. B **590**, 199 (2004). https://doi.org/10.1016/j.physletb.2004.02.040
9. G. Soyez, Saturation QCD predictions with heavy quarks at HERA. Phys. Lett. B **655**, 32 (2007). https://doi.org/10.1016/j.physletb.2007.07.076
10. K. Golec-Biernat, M. Wüsthoff, Saturation effects in deep inelastic scattering at low Q^2 and its implications on diffraction. Phys. Rev. D **59**, 014017 (1999). https://doi.org/10.1103/PhysRevD.59.014017
11. H.M. Wang, Z.Y. Hou, X.J. Sun, Hadron multiplicities in p+p and p+Pb collisions at the LHC. Nucl. Sci. Tech. **25**, 040502 (2014). https://doi.org/10.13538/j.1001-8042/nst.25.040502
12. Y.V. Kovchegov, Z. Lu, A.H. Rezaeian, Comparing AdS/CFT calculations to HERA F_2 data. Phys. Rev. D **80**, 074023 (2009). https://doi.org/10.1103/PhysRevD.80.074023
13. Y.V. Kovchegov, AdS/CFT applications to relativistic heavy-ion collisions: a brief review. Rep. Prog. Phys. **75**, 12 (2012). https://doi.org/10.1088/0034-4885/75/12/124301
14. D. Kharzeev, E. Levin, M. Nardi, QCD saturation and deuteron–nucleus collisions. Nucl. Phys. A **730**, 448 (2004). https://doi.org/10.1016/j.nuclphysa.2003.08.031
15. G. Karapetyan, The nuclear configurational entropy impact parameter dependence in the Color-Glass Condensate. EPL **118**, 38001 (2017). https://doi.org/10.1209/0295-5075/118/38001
16. G. Karapetyan, Fine-tuning the Color-Glass Condensate with the nuclear configurational entropy. EPL **117**, 18001 (2017). https://doi.org/10.1209/0295-5075/117/18001
17. A.E. Bernardini, R. da Rocha, Entropic information of dynamical AdS/QCD holographic models. Phys. Lett. B **762**, 107 (2016). https://doi.org/10.1016/j.physletb.2016.09.023
18. A.E. Bernardini, N.R.F. Braga, R. da Rocha, Configurational entropy of glueball states. Phys. Lett. B **765**, 81 (2017). https://doi.org/10.1016/j.physletb.2016.12.007
19. N.R.F. Braga, R. da Rocha, AdS/QCD duality and the quarkonia holographic information entropy. Phys. Lett. B **776**, 78 (2018). https://doi.org/10.1016/j.physletb.2017.11.034
20. N.R.F. Braga, R. da Rocha, Configurational entropy of anti-de Sitter black holes. Phys. Lett. B **767**, 386 (2017). https://doi.org/10.1016/j.physletb.2017.02.031
21. A. Dumitru, D.E. Kharzeev, E.M. Levin et al., Gluon saturation in pA collisions at energies available at the CERN Large Hadron Collider: predictions for hadron multiplicities. Phys. Rev. C **85**, 044920 (2012). https://doi.org/10.1103/PhysRevC.85.044920
22. H.M. Wang, J.F. Liu, Z.Y. Hou et al., Pseudo-rapidity distributions of charged hadrons in pp and pA collisions at the LHC. Chin. Phys. C **37**, 084102 (2013). https://doi.org/10.1088/1674-1137/37/8/084102
23. H. Fujii, K. Watanabe, Heavy quark pair production in high-energy pA collisions: Quarkonium. Nucl. Phys. A **915**, 1 (2013). https://doi.org/10.1016/j.nuclphysa.2013.06.011
24. S. Kretzer, H.L. Lai, F.I. Olness et al., CTEQ6 parton distributions with heavy quark mass effects. Phys. Rev. D **69**, 114005 (2004). https://doi.org/10.1103/PhysRevD.69.114005
25. J.L. Albacete, N. Armesto, J.G. Milhano et al., Nonlinear QCD meets data: a global analysis of lepton–proton scattering with running coupling Balitsky–Kovchegov evolution. Phys. Rev. D **80**, 034031 (2009). https://doi.org/10.1103/PhysRevD.80.034031
26. M.L. Miller, K. Reygers, S.J. Sanders et al., Glauber modeling in high-energy nuclear collisions. Annu. Rev. Nucl. Part. Sci. **57**, 205 (2007). https://doi.org/10.1146/annurev.nucl.57.090506.123020
27. C.W. Ma, Y.G. Ma, Shannon information entropy in heavy-ion collisions. Prog. Part. Nucl. Phys. **99**, 120 (2018). https://doi.org/10.1016/j.ppnp.2018.01.002
28. U. Heinz, J.S. Moreland, Energy dependent growth of the nucleon and hydrodynamic initial conditions. Phys. Rev. C **84**, 054905 (2011). https://doi.org/10.1103/PhysRevC.84.054905
29. H. Fujii, F. Gelis, R. Venugopalan, Quark pair production in high energy pA collisions: general features. Nucl. Phys. A **780**, 146 (2006). https://doi.org/10.1016/j.nuclphysa.2006.09.012
30. ALICE Collaboration, Measurement of quarkonium production at forward rapidity in pp collisions at $\sqrt{s}$ = 7 TeV. Eur. Phys. J. C **74**, 2974 (2014). https://doi.org/10.1140/epjc/s10052-014-2974-4
31. ALICE Collaboration, J/ψ production and nuclear effects in p-Pb collisions at $\sqrt{s_{\mathrm{NN}}}$ = 5.02 TeV. JHEP **1402**, 073 (2014). https://doi.org/10.1007/JHEP02(2014)073
32. LHCb Collaboration, Study of J/ψ production and cold nuclear matter effects in pPb collisions at $\sqrt{s_{NN}}$ = 5TeV. JHEP **1402**, 072 (2014). https://doi.org/10.1007/JHEP02(2014)072
33. ALICE Collaboration, Charmonium Production at forward rapidity in pp, p-Pb and Pb-Pb collisions, with ALICE. arXiv:1409.4458
34. LHCb Collaboration, Prompt and nonprompt J/ψ production and nuclear modification in pPb collisions at $\sqrt{s_{\mathrm{NN}}}$ = 8.16 TeV. Phys. Lett. B **774**, 159 (2017). https://doi.org/10.1016/j.physletb.2017.09.058